

# Robust control allocation for spacecraft attitude tracking under actuator faults

Qiang Shen, *Student Member, IEEE*, Danwei Wang, *Senior Member, IEEE*, Senqiang Zhu, and Eng Kee Poh

**Abstract**—This paper addresses attitude tracking problems for an overactuated spacecraft in the presence of actuator faults, imprecise fault estimation, and external disturbances. First, model reference adaptive control technique is used to design a high-level controller to produce the three-axis virtual control torque. Then, taking fault estimation uncertainties into account, a robust control allocation (RobCA) strategy is proposed to redistribute virtual control signals to the remaining actuators when an actuator fault occurs. The RobCA is formulated as a min-max optimization problem, which deals with actuator faults directly without reconfiguring the controller and ensures some robustness of system performances. Finally, Simulation results are provided to show the effectiveness of the overall control strategy.

**Index Terms**—Fault-tolerant control, actuators, control allocation, model reference adaptive control, attitude tracking.

## I. INTRODUCTION

FOR spacecraft attitude control systems, actuators play an important role in generating control efforts commanded from controller to achieve specific mission objectives. However, when a fault occurs in the actuator, the influence of controller on the spacecraft might be interrupted or modified. For example, the TOPEX satellite could not perform attitude maneuvers because of the failure of pitch reaction wheel, and its mission was finally aborted in October 2005 [1]. Therefore, to enhance the spacecraft reliability and safety, actuator fault tolerance capability needs to be addressed in attitude control design.

Depending on how redundancies are utilized, fault-tolerant control (FTC) solutions can be classified into two categories: passive and active strategies [2]. In passive FTC systems, all potential actuator faults are considered together with normal system operating conditions at the design stage, and a single fixed fault-tolerant controller is synthesized to achieve the given objectives. Several passive FTC methods have been proposed for spacecraft attitude control problem, such as indirect robust adaptive control [3], time-delay control with dynamic inversion [4], and adaptive sliding mode control [5], [6]. On the other hand, the active FTC approach reacts to actuator faults by reconfiguring the controller based on a fault detection and diagnosis (FDD) scheme which provides real-time information about faults, so that the desired performance is maintained in spite of actuator faults. In [7], actuator failure detection, identification and adaptive reconfigurable controller

for spacecraft were proposed. In [8], an iterative learning observer was designed to estimate time-varying actuator faults. Based on the FDD scheme developed in [8], an FTC law was reconfigured in [9] to accomplish attitude stabilization under partial loss of actuator effectiveness faults. In [10], the problem of nonlinear fault detection, isolation, and recovery for the spacecraft orbital and attitude control system was investigated. In [11], based on reconstructed fault information from a terminal sliding mode observer, a fault compensation control law was developed for spacecraft to follow the desired attitude trajectories after a finite settling time.

Modern spacecraft often uses redundant actuators to enhance the reliability, maneuverability and survivability. This makes the spacecraft attitude control system an over-actuated system, which has more control effects than three conventional control effectors [12]. Due to this redundancy, control allocation is utilized to distribute the desired total control demand over the individual actuators, especially in case of actuator faults [13], [14]. In [15]–[17], sliding mode control and non-robust control allocation were combined for FTC to handle actuator faults in flight control systems. In [18], a robust least-squares control allocation was proposed for flight control system when the control effectiveness matrix is subject to uncertainties/faults. In particular, for spacecraft attitude control systems, a velocity-free nonlinear proportional-integral controller was designed in [19] as a high-level controller and a robust control allocation was used to distribute the three-axis moments over the available actuators.

In this paper, a model reference adaptive (MRA) high-level controller incorporating robust control allocation (RobCA) scheme is proposed for spacecraft attitude tracking under actuator faults, imprecise FDD, and external disturbances. The main contributions of this paper are summarized as follows.

- 1) The external disturbances can be rejected by the MRA high-level controller without considering actuator faults, and the closed-loop performance is defined by a reference model, which creates a desired trajectory for the attitude tracking system to follow.
- 2) In contrast to the existing control allocation based FTC schemes such as [15], [16], imprecise fault estimation in both actuator effectiveness and additive fault is considered. Moreover, the proposed methods ensure robustness of system performances with respect to imprecise fault estimation in control allocation design instead of in high-level controller design. Therefore, design complexity of the high-level controller can be reduced.
- 3) Comparing with aforementioned robust control allocation methods such as [18], [19], the optimal index of

The authors are with the School of Electrical and Electronic Engineering, Nanyang Technological University, Singapore 639798, Singapore (e-mail: qshen1@e.ntu.edu.sg; edwwang@ntu.edu.sg; sqzhu@ntu.edu.sg; eekpoh@ntu.edu.sg).

minimizing the energy consumption is introduced to guarantee that the solution is unique in both unsaturated and saturated cases of RobCA. Furthermore, to reduce computation burden in the unsaturated case of RobCA, the original vector optimization problem is converted to a one-dimensional search problem.

The remainder of this paper is organized as follows. In Section II, the mathematic models for spacecraft attitude tracking systems and actuator faults are presented. In Section III, the MRA high-level controller is designed. In Section IV, the solutions for unsaturated RobCA problem and saturated RobCA problem are presented. Section V illustrates the application of the overall control strategy to a rigid spacecraft, followed by conclusions in Section VI.

## II. SYSTEM DESCRIPTION AND PROBLEM STATEMENT

### A. Spacecraft Attitude Dynamics

The kinematics and dynamics for attitude motion of a rigid spacecraft can be expressed by the following equations [20]:

$$\begin{cases} \mathbf{J}\dot{\boldsymbol{\omega}} = -\boldsymbol{\omega}^\times \mathbf{J}\boldsymbol{\omega} + \mathbf{D}\mathbf{u} + \mathbf{d} \\ \dot{\mathbf{q}} = \frac{1}{2}(\mathbf{q}^\times + q_0 \mathbf{I}_3)\boldsymbol{\omega} \\ \dot{q}_0 = -\frac{1}{2}\mathbf{q}^T \boldsymbol{\omega}, \end{cases} \quad (1)$$

where  $\mathbf{J} \in \mathbb{R}^{3 \times 3}$  denotes the positive definite inertia matrix of the spacecraft,  $\boldsymbol{\omega} \in \mathbb{R}^3$  is the inertial angular velocity vector of the spacecraft with respect to an inertial frame  $\mathcal{I}$  and expressed in the body frame  $\mathcal{B}$ ,  $\mathbf{Q} = [q_1 \ q_2 \ q_3 \ q_0]^T = [\mathbf{q}^T \ q_0]^T \in \mathbb{R}^3 \times \mathbb{R}$  denotes the unit quaternion describing the attitude orientation of the body frame  $\mathcal{B}$  with respect to inertial frame  $\mathcal{I}$  and satisfies the constraint  $\mathbf{q}^T \mathbf{q} + q_0^2 = 1$ ,  $\mathbf{I}_3 \in \mathbb{R}^{3 \times 3}$  denotes a 3-by-3 identity matrix,  $\mathbf{u} \in \mathbb{R}^n$  ( $n > 3$ ) denotes the control torque produced by  $n$  actuators, and  $\mathbf{D} \in \mathbb{R}^{3 \times n}$  is the actuator distribution matrix, the notation  $\mathbf{x}^\times \in \mathbb{R}^{3 \times 3}$  for a vector  $\mathbf{x} = [x_1 \ x_2 \ x_3]^T$  is used to represent the skew-symmetric cross-product matrix.

The external disturbances  $\mathbf{d}(t) = [d_1(t) \ d_2(t) \ d_3(t)]^T \in \mathbb{R}^3$  may come in many forms, and they are considered in this paper as a combination of a constant and a series of sinusoidal functions [21], [22], i.e., each component  $d_i(t)$ ,  $i \in \{1, 2, 3\}$ , is given by

$$d_i(t) = h_{i0} + \sum_{j=1}^{n_i} h_{ij} \sin(\omega_{ij}t + \Upsilon_{ij}) \quad (2)$$

where  $h_{i0}$  and  $h_{ij}$  are arbitrarily unknown amplitudes,  $\Upsilon_{ij}$  are unknown phase angles, and  $\omega_{ij}$  are known frequencies. Therefore, the disturbance model (2) can be written in a compact form:

$$d_i(t) = \mathbf{H}_i^T \boldsymbol{\Psi}_i(t) \quad (3)$$

where  $\mathbf{H}_i = [h_{i0} \ h_{i1} \cos\Upsilon_{i1} \ \cdots \ h_{in_i} \cos\Upsilon_{in_i} \ h_{i1} \sin\Upsilon_{i1} \ \cdots \ h_{in_i} \sin\Upsilon_{in_i}]^T \in \mathbb{R}^{2n_i+1}$  is an unknown vector with constant elements, and  $\boldsymbol{\Psi}_i(t) = [1 \ \sin(\omega_{i1}t) \ \cdots \ \sin(\omega_{in_i}t) \ \cos(\omega_{i1}t) \ \cdots \ \cos(\omega_{in_i}t)]^T \in \mathbb{R}^{2n_i+1}$  is known.

In the fault-free case, the actual output torque  $\mathbf{u}$  of  $n$  actuators is equal to the desired value  $\mathbf{u}_c$  commanded by

controller, i.e.,  $\mathbf{u} = \mathbf{u}_c$ . When actuator faults are considered, faults of  $n$  actuators are modelled as follows:

$$\mathbf{u} = \mathbf{E}\mathbf{u}_c + \bar{\mathbf{u}}, \quad (4)$$

where  $\mathbf{u}_c = [u_{c1} \ u_{c2} \ \cdots \ u_{cn}]^T \in \mathbb{R}^n$  denotes the command control torque,  $\mathbf{E} = \text{diag}\{e_1, e_2, \dots, e_n\} \in \mathbb{R}^{n \times n}$  denotes the effectiveness factor matrix of spacecraft actuators with  $0 \leq e_i \leq 1$ ,  $i \in \{1, 2, \dots, n\}$ . Note that the case  $e_i = 1$  indicates that the  $i$ th actuator works normally, and  $0 < e_i < 1$  implies that the  $i$ th actuator partially loses its effectiveness, but still does not totally fail. The value  $e_i = 0$  means that the  $i$ th actuator undergoes a complete failure. To ensure three-axis attitude control, it is assumed that up to  $n - 3$  actuators can suffer from total failure simultaneously. The vector  $\bar{\mathbf{u}} = [\bar{u}_1 \ \bar{u}_2 \ \cdots \ \bar{u}_n]^T \in \mathbb{R}^n$  represents the bounded additive fault. Hence, the nonlinear attitude kinetics model incorporating actuator faults can be rewritten in the following form:

$$\mathbf{J}\dot{\boldsymbol{\omega}} = -\boldsymbol{\omega}^\times \mathbf{J}\boldsymbol{\omega} + \mathbf{D}(\mathbf{E}\mathbf{u}_c + \bar{\mathbf{u}}) + \mathbf{d}. \quad (5)$$

### B. Attitude Error Dynamics

To address the attitude tracking issue, the desired attitude and the desired angular velocity of the spacecraft in the desired reference frame  $\mathcal{B}_d$  with respect to inertial frame  $\mathcal{I}$  are denoted by unit quaternion  $\mathbf{Q}_d = [q_d^T \ q_{d0}]^T$  and  $\boldsymbol{\omega}_d$ , respectively. The attitude tracking error  $\mathbf{Q}_e = [q_e^T \ q_{e0}]^T$  is defined as the relative orientation between attitude  $\mathbf{Q}$  and target attitude  $\mathbf{Q}_d$ , which is computed as  $\mathbf{Q}_e = \mathbf{Q}_d^{-1} \otimes \mathbf{Q}$ , where  $\mathbf{Q}_d^{-1}$  is the inverse or conjugate of the desired quaternion determined by  $\mathbf{Q}_d^{-1} = [-q_d^T \ q_{d0}]^T$ , and  $\otimes$  denotes the quaternion multiplication operator of two unit quaternion  $\mathbf{Q}_i = [q_i^T \ q_{i0}]^T$  and  $\mathbf{Q}_j = [q_j^T \ q_{j0}]^T$ , which is defined as follows:

$$\mathbf{Q}_i \otimes \mathbf{Q}_j = \begin{bmatrix} q_{i0}q_j + q_{j0}q_i + \mathbf{q}_i^\times \mathbf{q}_j \\ q_{i0}q_{j0} - \mathbf{q}_i^T \mathbf{q}_j \end{bmatrix}. \quad (6)$$

The angular velocity error  $\boldsymbol{\omega}_e \in \mathbb{R}^3$  is given by  $\boldsymbol{\omega}_e = \boldsymbol{\omega} - \mathbf{C}\boldsymbol{\omega}_d$ , where  $\mathbf{C}$  is the rotation matrix, which is defined as  $\mathbf{C} = (q_{e0}^2 - \mathbf{q}_e^T \mathbf{q}_e) \mathbf{I}_3 + 2\mathbf{q}_e \mathbf{q}_e^T - 2q_{e0} \mathbf{q}_e^\times$ . Consequently, based on the attitude dynamics in (5), the attitude tracking error system with actuator faults can be described as

$$\begin{cases} \mathbf{J}\dot{\boldsymbol{\omega}}_e = -(\boldsymbol{\omega}_e + \mathbf{C}\boldsymbol{\omega}_d)^\times \mathbf{J}(\boldsymbol{\omega}_e + \mathbf{C}\boldsymbol{\omega}_d) \\ \quad + \mathbf{J}(\boldsymbol{\omega}_e^\times \mathbf{C}\boldsymbol{\omega}_d - \mathbf{C}\dot{\boldsymbol{\omega}}_d) + \mathbf{D}(\mathbf{E}\mathbf{u}_c + \bar{\mathbf{u}}) + \mathbf{d} \\ \dot{\mathbf{q}}_e = \frac{1}{2}(\mathbf{q}_e^\times + q_{e0} \mathbf{I}_3)\boldsymbol{\omega}_e \\ \dot{q}_{e0} = -\frac{1}{2}\mathbf{q}_e^T \boldsymbol{\omega}_e. \end{cases} \quad (7)$$

*Assumption 1:* The inertia matrix  $\mathbf{J}$  is a symmetric, positive definite and bounded constant matrix. There exists a positive constant  $c_J$  such that  $\mathbf{x}^T \mathbf{J} \mathbf{x} \leq c_J \|\mathbf{x}\|^2$  for any  $\mathbf{x} \in \mathbb{R}^3$ . The notation  $\|\cdot\|$  denotes the Euclidean norm or its induced norm.

*Assumption 2:* The desired angular velocity of spacecraft and its time derivative (i.e.,  $\boldsymbol{\omega}_d$  and  $\dot{\boldsymbol{\omega}}_d$ ) are bounded.

### C. Problem Statement

For overactuated systems, it is possible to divide the controller design into two steps [23]. The overall structure of the proposed FTC attitude tracking scheme is shown in Fig. 1.

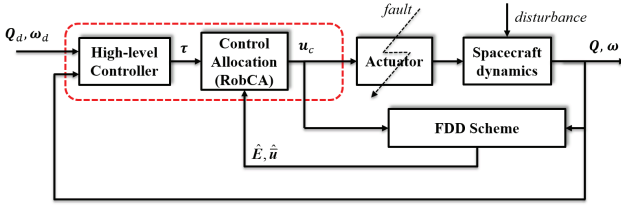


Fig. 1. Structure of the overall proposed FTC system.

### Step 1: High-level Controller Design

In the first step, the virtual control torque  $\tau \in \mathbb{R}^3$  is designed to specify total attitude control torque, which is introduced as

$$\tau = D\mathbf{u} = D(\mathbf{E}u_c + \bar{\mathbf{u}}). \quad (8)$$

As a result, the attitude tracking error dynamics in (7) can be rewritten as the following virtual equivalent system

$$\begin{cases} \mathbf{J}\dot{\boldsymbol{\omega}}_e = -(\boldsymbol{\omega}_e + \mathbf{C}\boldsymbol{\omega}_d)^\times \mathbf{J}(\boldsymbol{\omega}_e + \mathbf{C}\boldsymbol{\omega}_d) \\ \quad + \mathbf{J}(\boldsymbol{\omega}_e^\times \mathbf{C}\boldsymbol{\omega}_d - \mathbf{C}\dot{\boldsymbol{\omega}}_d) + \tau + \mathbf{d} \\ \dot{\mathbf{q}}_e = \frac{1}{2}(\mathbf{q}_e^\times + q_{e0}\mathbf{I}_3)\boldsymbol{\omega}_e \\ \dot{q}_{e0} = -\frac{1}{2}\mathbf{q}_e^T \boldsymbol{\omega}_e. \end{cases} \quad (9)$$

### Step 2: Control Allocation Design

In the second step, with consideration of the imprecision in FDD, a RobCA algorithm is designed to distribute the desired total control commands determined by the high-level controller equivalently to each individual actuator.

## III. HIGH-LEVEL CONTROLLER DESIGN

In this section, an MRA high-level controller is proposed for the spacecraft attitude tracking system in the presence of external disturbances. Define a lumped error variable [24]

$$\mathbf{s} = \boldsymbol{\omega}_e + \beta \mathbf{q}_e, \quad (10)$$

where  $\beta$  is a positive constant. Then, from (9), the dynamic equation for the lumped error variable  $\mathbf{s}$  is obtained as

$$\mathbf{J}\dot{\mathbf{s}} = \mathbf{f}(\boldsymbol{\omega}, \boldsymbol{\omega}_d, \dot{\boldsymbol{\omega}}_d, \mathbf{Q}, \mathbf{Q}_d) + \tau + \mathbf{d}, \quad (11)$$

where  $\mathbf{f}(\boldsymbol{\omega}, \boldsymbol{\omega}_d, \dot{\boldsymbol{\omega}}_d, \mathbf{Q}, \mathbf{Q}_d) \in \mathbb{R}^3$  is given by

$$\begin{aligned} \mathbf{f} = & -(\boldsymbol{\omega}_e + \mathbf{C}\boldsymbol{\omega}_d)^\times \mathbf{J}(\boldsymbol{\omega}_e + \mathbf{C}\boldsymbol{\omega}_d) \\ & + \frac{\beta}{2}\mathbf{J}(\mathbf{q}_e^\times + q_{e0}\mathbf{I}_3)\boldsymbol{\omega}_e + \mathbf{J}(\boldsymbol{\omega}_e^\times \mathbf{C}\boldsymbol{\omega}_d - \mathbf{C}\dot{\boldsymbol{\omega}}_d). \end{aligned} \quad (12)$$

To obtain the online information on disturbances, an auxiliary system that can be regarded as a reference model to the lumped error dynamics (11), is introduced as

$$\mathbf{J}\dot{\hat{\mathbf{s}}} = \mathbf{f} + \boldsymbol{\chi} + \hat{\mathbf{d}}(t), \quad (13)$$

where  $\hat{\mathbf{s}} = [\hat{s}_1 \ \hat{s}_2 \ \hat{s}_3]^T \in \mathbb{R}^3$  is the estimate of lumped error variable,  $\boldsymbol{\chi} \in \mathbb{R}^3$  is the input of the auxiliary system that will be given later. The vector  $\hat{\mathbf{d}}(t) = [\hat{\mathbf{H}}_1^T \boldsymbol{\Psi}_1(t) \ \hat{\mathbf{H}}_2^T \boldsymbol{\Psi}_2(t) \ \hat{\mathbf{H}}_3^T \boldsymbol{\Psi}_3(t)]^T \in \mathbb{R}^3$  denotes the estimate of the disturbance, where  $\hat{\mathbf{H}}_i \in \mathbb{R}^{2n_i+1}$ ,  $i \in \{1, 2, 3\}$ , is the estimate of  $\mathbf{H}_i$  in (2).

Define the reference model tracking error as  $\tilde{\mathbf{s}} = [\tilde{s}_1 \ \tilde{s}_2 \ \tilde{s}_3]^T \in \mathbb{R}^3$  with  $\tilde{s}_i = \hat{s}_i - s_i$ ,  $i \in \{1, 2, 3\}$ . Then, dynamics for  $\tilde{\mathbf{s}}$  is written as

$$\mathbf{J}\dot{\tilde{\mathbf{s}}} = \boldsymbol{\chi} - \tau + \tilde{\mathbf{d}}(t), \quad (14)$$

where  $\tilde{\mathbf{d}}(t) = [\tilde{\mathbf{H}}_1^T \boldsymbol{\Psi}_1(t) \ \tilde{\mathbf{H}}_2^T \boldsymbol{\Psi}_2(t) \ \tilde{\mathbf{H}}_3^T \boldsymbol{\Psi}_3(t)]^T \in \mathbb{R}^3$  with  $\tilde{\mathbf{H}}_i = \hat{\mathbf{H}}_i - \mathbf{H}_i$ ,  $i \in \{1, 2, 3\}$ , is the disturbance estimate error.

Next, the theorem with regard to the MRA high-level controller is stated as follows:

*Theorem 1:* Consider that the attitude tracking error dynamics is described by (9) with external disturbances given in (2) and that assumptions 1-2 are satisfied. Define the MRA high-level controller as

$$\tau = \boldsymbol{\chi} + k_1 \tilde{\mathbf{s}} - k_3 \mathbf{q}_e \quad (15)$$

with  $\boldsymbol{\chi}$  given by

$$\boldsymbol{\chi} = -\hat{\mathbf{d}}(t) - \mathbf{f} - k_2 \hat{\mathbf{s}}, \quad (16)$$

where  $k_1$ ,  $k_2$ , and  $k_3$  are positive constant gains, and  $k_2$  and  $k_3$  are chosen so that  $4\beta k_2 > k_3$ . Let the adaptive law for  $\hat{\mathbf{H}}_i$  in  $\hat{\mathbf{d}}(t)$  of (16) be updated by

$$\dot{\hat{\mathbf{H}}}_i(t) = -\boldsymbol{\Lambda}_i \boldsymbol{\Psi}_i(t) \tilde{s}_i, \quad (17)$$

where  $\boldsymbol{\Lambda}_i$  is a diagonal matrix with positive entries. Then, the closed-loop attitude tracking error system will converge to the equilibrium point  $\mathbf{Q}_e = [\mathbf{q}_e^T \ q_{e0}]^T = [1 \ 0]^T$ ,  $\boldsymbol{\omega}_e = 0$  asymptotically.

*Proof.* Consider the following candidate Lyapunov function:

$$\begin{aligned} V = & \frac{1}{2} \tilde{\mathbf{s}}^T \mathbf{J} \tilde{\mathbf{s}} + \frac{1}{2} \hat{\mathbf{s}}^T \mathbf{J} \hat{\mathbf{s}} + k_3 [\mathbf{q}_e^T \mathbf{q}_e + (1 - q_{e0})^2] \\ & + \frac{1}{2} \sum_{i=1}^3 \tilde{\mathbf{H}}_i^T \boldsymbol{\Lambda}_i^{-1} \tilde{\mathbf{H}}_i. \end{aligned} \quad (18)$$

Differentiating  $V$  along trajectories of (13) and (14) results in

$$\begin{aligned} \dot{V} = & \tilde{\mathbf{s}}^T (\boldsymbol{\chi} - \tau + \tilde{\mathbf{d}}) + \hat{\mathbf{s}}^T (\mathbf{f} + \boldsymbol{\chi} + \hat{\mathbf{d}}) \\ & + k_3 \mathbf{q}_e^T \mathbf{s} - \beta k_3 \|\mathbf{q}_e\|^2 + \sum_{i=1}^3 \tilde{\mathbf{H}}_i^T \boldsymbol{\Lambda}_i^{-1} \dot{\tilde{\mathbf{H}}}_i. \end{aligned}$$

Since  $\mathbf{H}_i$  is a vector with constant elements, it follows that  $\tilde{\mathbf{H}}_i = \dot{\hat{\mathbf{H}}}_i$ . Substituting the high-level controller given in (15) and (16) and adaptive law given by (17) into above yields

$$\begin{aligned} \dot{V} \leq & -k_1 \|\tilde{\mathbf{s}}\|^2 - k_2 \|\hat{\mathbf{s}}\|^2 + k_3 \hat{\mathbf{s}}^T \mathbf{q}_e - \beta k_3 \|\mathbf{q}_e\|^2 \\ & + \tilde{\mathbf{s}}^T \tilde{\mathbf{d}} - \sum_{i=1}^3 \tilde{\mathbf{H}}_i^T \boldsymbol{\Psi}_i(t) \tilde{s}_i \\ \leq & -k_1 \|\tilde{\mathbf{s}}\|^2 - [\hat{\mathbf{s}}^T \ \mathbf{q}_e^T] \mathbf{P} [\hat{\mathbf{s}}^T \ \mathbf{q}_e^T]^T, \end{aligned} \quad (19)$$

where  $\mathbf{P} = \begin{bmatrix} k_2 \mathbf{I}_3 & -\frac{1}{2} k_3 \mathbf{I}_3 \\ -\frac{1}{2} k_3 \mathbf{I}_3 & \beta k_3 \mathbf{I}_3 \end{bmatrix}$ .

Since  $4\beta k_2 > k_3$ , it is clear that  $\mathbf{P}$  is positive definite, which implies that  $V$  is nonincreasing and bounded for all  $t \geq 0$ , and it follows that  $\tilde{\mathbf{s}}$ ,  $\hat{\mathbf{s}}$ ,  $\mathbf{q}_e$ , and  $\hat{\mathbf{H}}_i$  are all bounded. As  $\tilde{\mathbf{s}}$  and  $\hat{\mathbf{s}}$  are bounded, it is clear that the lumped error variable  $\mathbf{s}$  is bounded for all  $t \geq 0$ , which implies that  $\boldsymbol{\omega}_e$  is bounded due to the boundedness of  $\mathbf{q}_e$ . Consequently, using

assumptions 1-2 and boundedness of  $\omega_e$  and  $\widetilde{H}_i$ , one can show that  $\mathbf{f}(\boldsymbol{\omega}, \boldsymbol{\omega}_d, \dot{\boldsymbol{\omega}}_d, \mathbf{Q}, \mathbf{Q}_d)$  and  $\hat{\mathbf{d}}$  are bounded for all  $t \geq 0$ . Since  $\hat{\mathbf{d}}$ ,  $\mathbf{f}$ , and  $\hat{\mathbf{s}}$  are bounded, it is clear from (16) that  $\boldsymbol{\chi}$  is bounded, and hence one can conclude that  $\boldsymbol{\tau}$  is also bounded for all  $t \geq 0$ . Therefore, from (13), (14), and second equation of (9), one can easily verify that  $\hat{\mathbf{s}}$ ,  $\dot{\hat{\mathbf{s}}}$ , and  $\dot{\mathbf{q}}_e$  are bounded for all  $t \geq 0$ , which implies that  $\hat{\mathbf{s}}$ ,  $\tilde{\mathbf{s}}$ , and  $\mathbf{q}_e$  are uniformly continuous functions. Moreover, from (19), it is easy to verify that  $\hat{\mathbf{s}}$ ,  $\tilde{\mathbf{s}}$ ,  $\mathbf{q}_e \in \ell_2$ . Then, from the Barbalat's Lemma (using the alternative statement of this lemma from *Corollary A.7* of [25]), it yields that  $\tilde{\mathbf{s}} \rightarrow 0$ ,  $\hat{\mathbf{s}} \rightarrow 0$ , and  $\mathbf{q}_e \rightarrow 0$  as  $t \rightarrow \infty$ . Hence, from  $\tilde{\mathbf{s}} \rightarrow 0$  and  $\hat{\mathbf{s}} \rightarrow 0$ , one can conclude that  $\mathbf{s} \rightarrow 0$ . Since  $\mathbf{s} \rightarrow 0$  and  $\mathbf{q}_e \rightarrow 0$ , it follows from (10) that  $\boldsymbol{\omega}_e \rightarrow 0$  as well. Moreover, since  $\mathbf{q}_e \rightarrow 0$  and  $\mathbf{q}_e^2 + \mathbf{q}_{e0}^2 = 1$ , it leads to  $\mathbf{q}_{e0} \rightarrow \pm 1$ . As discussed in [26] that  $\mathbf{q}_{e0} = -1$  is not a stable equilibrium, it is obtained that  $\mathbf{q}_{e0} \rightarrow 1$  as  $t \rightarrow \infty$ . Therefore, the result in Theorem 1 is established.  $\square$

*Remark 1:* The introduction of the auxiliary system (13) provides a reference model for the lumped error system (11) to follow. In fact, by substituting the auxiliary system input (16) in (13), it is obtained that  $\mathbf{J}\dot{\hat{\mathbf{s}}} = -k_2\hat{\mathbf{s}}$ . Consequently, one can choose a candidate Lyapunov function  $V = \frac{1}{2}\hat{\mathbf{s}}^T \mathbf{J}\hat{\mathbf{s}}$ , and it is proved that  $\hat{\mathbf{s}}$  converge to zero with an exponential rate greater than  $\frac{2k_2}{c_J}$  by Lyapunov stability analysis. This state trajectory of the auxiliary system creates a desired reference trajectory for the state of the lumped error system to follow.

*Remark 2:* From (19) and Remark 1, it is obtained that larger  $k_1$ ,  $k_2$ , and  $\beta$  yield a faster convergence of  $\tilde{\mathbf{s}}$ ,  $\hat{\mathbf{s}}$ , and  $\mathbf{q}_e$ , respectively. However, to ensure asymptotic stability of the closed-loop attitude tracking system, the condition  $4\beta k_2 > k_3$  should be satisfied firstly (i.e., make sure that matrix  $\mathbf{P}$  in (19) is positive-definite).

#### IV. CONTROL ALLOCATION DESIGN

Due to physical limitations on actuators, the amplitude and rate constraints of actuators are considered in the control allocation design. For simplicity, it is assumed that the actuators have the same amplitude and rate constraint values, and the command control inputs  $\mathbf{u}_c$  are restricted by

$$\delta_{min} \leq u_{ci} \leq \delta_{max}, \quad |\dot{u}_{ci}| \leq \eta_{rate} \quad (20)$$

where lower and upper position constraints of the  $i$ th actuator are defined by  $\delta_{min}$  and  $\delta_{max}$ , respectively, and  $\eta_{rate}$  is the maximum control rate of the  $i$ th actuator. Because modern spacecraft attitude control systems are implemented in a digital computer, rate constraints can be converted into position constraints. Then, overall constraints are further specified as

$$\underline{\mathbf{u}}_c \leq \mathbf{u}_c \leq \bar{\mathbf{u}}_c, \quad (21)$$

with  $\underline{u}_{ci} = \max\{\delta_{min}, u_{ci}(t - T) - T\eta_{rate}\}$  and  $\bar{u}_{ci} = \min\{\delta_{max}, u_{ci}(t - T) + T\eta_{rate}\}$ , where  $\underline{\mathbf{u}}_c = [\underline{u}_{c1} \ \underline{u}_{c2} \ \cdots \ \underline{u}_{cn}]^T \in \mathbb{R}^n$  and  $\bar{\mathbf{u}}_c = [\bar{u}_{c1} \ \bar{u}_{c2} \ \cdots \ \bar{u}_{cn}]^T \in \mathbb{R}^n$  are the combined constraints for  $n$  actuators,  $T$  is the sampling time, and  $u_{ci}(t - T)$  is the  $i$ th command control input in the previous sampling instant.

In addition, in order to handle actuator faults, estimated fault information is used in control allocation. Assuming that

actuator fault information,  $\hat{\mathbf{E}} = \text{diag}\{\hat{e}_1, \hat{e}_2, \dots, \hat{e}_n\} \in \mathbb{R}^{n \times n}$  and  $\hat{\mathbf{u}} = [\hat{u}_1 \ \hat{u}_2 \ \cdots \ \hat{u}_n]^T \in \mathbb{R}^n$ , is detected and estimated by an FDD scheme. However, no matter which FDD scheme is employed, it is inevitable to have some estimation or identification errors [15], and  $\hat{\mathbf{E}}$  and  $\hat{\mathbf{u}}$  may not be identical to their actual values. Hence, the level of imprecision of fault estimation is introduced. Relations between actual fault and their estimated values are assumed to satisfy

$$\mathbf{E} = (\mathbf{I}_n - \boldsymbol{\Delta}_E)\hat{\mathbf{E}}, \quad \bar{\mathbf{u}} = (\mathbf{I}_n - \boldsymbol{\Delta}_{\bar{\mathbf{u}}})\hat{\mathbf{u}}, \quad (22)$$

where  $\boldsymbol{\Delta}_E = \text{diag}\{\delta_{e1} \ \delta_{e2} \ \cdots \ \delta_{en}\} \in \mathbb{R}^{n \times n}$  and  $\boldsymbol{\Delta}_{\bar{\mathbf{u}}} = \text{diag}\{\delta_{\bar{u}1} \ \delta_{\bar{u}2} \ \cdots \ \delta_{\bar{u}n}\} \in \mathbb{R}^n$ , and the unknown scalars  $\delta_{ei}$  and  $\delta_{\bar{u}i}$  represent the level of imprecision in the estimation of actuator effectiveness and additive fault, respectively. Thus, during the control allocation, the command control efforts  $\mathbf{u}_c$  in (8) need to be found such that

$$\boldsymbol{\tau} = \mathbf{D}[(\mathbf{I}_n - \boldsymbol{\Delta}_E)\hat{\mathbf{E}}\mathbf{u}_c + (\mathbf{I}_n - \boldsymbol{\Delta}_{\bar{\mathbf{u}}})\hat{\mathbf{u}}]. \quad (23)$$

In light of uncertainties in (23), RobCA is formulated as

$$\mathbf{u}_c = \arg \min_{\underline{\mathbf{u}}_c \leq \mathbf{u}_c \leq \bar{\mathbf{u}}_c} \max_{\substack{\|\boldsymbol{\Delta}_E\| \leq \rho_1, \\ \|\boldsymbol{\Delta}_{\bar{\mathbf{u}}}\| \leq \rho_2}} \left\{ \|\mathbf{u}_c\|_M^2 + h \|\mathbf{D}(\mathbf{I}_n - \boldsymbol{\Delta}_E)\hat{\mathbf{E}}\mathbf{u}_c + \mathbf{D}(\mathbf{I}_n - \boldsymbol{\Delta}_{\bar{\mathbf{u}}})\hat{\mathbf{u}} - \boldsymbol{\tau}\|^2 \right\}, \quad (24)$$

where  $\|\mathbf{u}_c\|_M^2$  stands for  $\mathbf{u}_c^T \mathbf{M} \mathbf{u}_c$ , the weighting matrix  $\mathbf{M}$  is positive-definite, the constant  $h > 0$ ,  $\rho_1$  and  $\rho_2$  are two known positive scalars such that  $\|\boldsymbol{\Delta}_E\| \leq \rho_1$  and  $\|\boldsymbol{\Delta}_{\bar{\mathbf{u}}}\| \leq \rho_2$ , respectively.

For the RobCA in (24), the primary objective represented by the second term is to find the optimal  $\mathbf{u}_c$  by minimizing the worse-case residual. This achieves some robustness given by the worst residual to control allocation with respect to the imprecision in the fault estimation of the FDD scheme [18], [27]. Comparing with the results in [18], [19], since there is no guarantee that  $\boldsymbol{\tau}$  is attainable or that the solution of  $\mathbf{u}_c$  is unique, a secondary objective of RobCA represented by the first term in (24), which minimizes the commanded power consumption, is also considered.

To reduce the notational burden, let  $\mathbf{A} = \mathbf{D}\hat{\mathbf{E}}$ ,  $\mathbf{b} = \boldsymbol{\tau} - \mathbf{D}\hat{\mathbf{u}}$ ,  $\boldsymbol{\Delta}\mathbf{A} = -\mathbf{D}\boldsymbol{\Delta}_E\hat{\mathbf{E}}$ , and  $\boldsymbol{\Delta}\mathbf{b} = \mathbf{D}\boldsymbol{\Delta}_{\bar{\mathbf{u}}}\hat{\mathbf{u}}$ . Then, we get that  $\|\boldsymbol{\Delta}\mathbf{A}\| \leq \rho_A$ ,  $\|\boldsymbol{\Delta}\mathbf{b}\| \leq \rho_b$ , where  $\rho_A = \rho_1 \|\mathbf{D}\| \|\hat{\mathbf{E}}\|$ ,  $\rho_b = \rho_2 \|\mathbf{D}\| \|\hat{\mathbf{u}}\|$ . Thus, the proposed RobCA becomes

$$\mathbf{u}_c = \arg \min_{\underline{\mathbf{u}}_c \leq \mathbf{u}_c \leq \bar{\mathbf{u}}_c} \left\{ \|\mathbf{u}_c\|_M^2 + \max_{\substack{\|\boldsymbol{\Delta}\mathbf{A}\| \leq \rho_A, \\ \|\boldsymbol{\Delta}\mathbf{b}\| \leq \rho_b}} h \|(\mathbf{A} + \boldsymbol{\Delta}\mathbf{A})\mathbf{u}_c - (\mathbf{b} + \boldsymbol{\Delta}\mathbf{b})\|^2 \right\}. \quad (25)$$

In the following, the proposed RobCA problem is studied for both unsaturated and saturated actuators.

##### A. Unsaturated Case

When no actuator saturates, actuator constraints can be disregarded. Furthermore, it is verified that the unsaturated RobCA problem is equivalent to the following problem [28]

$$\mathbf{u}_c = \arg \min_{\mathbf{u}_c} \left\{ \|\mathbf{u}_c\|_M^2 + \max_{\|z\| \leq \phi(\mathbf{u}_c)} h \|\mathbf{A}\mathbf{u}_c - \mathbf{b} + z\|^2 \right\} \quad (26)$$

where  $\mathbf{z} = \mathbf{\Delta A} \mathbf{u}_c - \mathbf{\Delta b}$ ,  $\phi(\mathbf{u}_c)$  is defined as  $\phi(\mathbf{u}_c) = \rho_A \|\mathbf{u}_c\| + \rho_b$ .

To solve (26), the inner maximization problem is solved first, then followed by the outer minimization problem. For the inner maximization problem, the maximum

$$L(\mathbf{u}_c) \triangleq \max_{\|\mathbf{z}\| \leq \phi(\mathbf{u}_c)} h \|\mathbf{A} \mathbf{u}_c - \mathbf{b} + \mathbf{z}\|^2 \quad (27)$$

is convex in  $\mathbf{u}_c$ , and the inequality constraint is also convex in  $\mathbf{z}$ , so the maximum over  $\mathbf{z}$  is achieved at the boundary, i.e.,  $\|\mathbf{z}\| = \phi(\mathbf{u}_c)$ . Introducing a nonnegative Lagrange multiplier  $\lambda$ , the constrained maximization problem in (27) is transformed into the following unconstrained problem

$$L(\mathbf{u}_c) = \max_{\mathbf{z}, \lambda} \left[ h \|\mathbf{A} \mathbf{u}_c - \mathbf{b} + \mathbf{z}\|^2 - \lambda (\|\mathbf{z}\|^2 - \phi^2(\mathbf{u}_c)) \right]. \quad (28)$$

Differentiating (28) with respect to  $\mathbf{z}$  and  $\lambda$  yields

$$(\lambda^* - h) \mathbf{z}^* = h(\mathbf{A} \mathbf{u}_c - \mathbf{b}), \quad \|\mathbf{z}^*\| = \phi(\mathbf{u}_c), \quad (29)$$

where  $\mathbf{z}^*$  and  $\lambda^*$  denote the optimal solution of the maximization problem in (28). Computing the Hessian of  $L(\mathbf{u}_c)$  with respect to  $\mathbf{z}$ , and let it be positive-definite when  $\lambda = \lambda^*$ . Then, it can be found that  $\lambda^*$  should satisfy  $\lambda^* > h$ . In view of (29), the maximum cost in (28) is given by

$$L(\mathbf{u}_c) = \frac{h\lambda^*}{\lambda^* - h} \|\mathbf{A} \mathbf{u}_c - \mathbf{b}\|^2 + \lambda^* \phi^2(\mathbf{u}_c). \quad (30)$$

Substituting (30) into the original problem (26), the unsaturated RobCA problem is equivalent to the following minimization problem:

$$\mathbf{u}_c = \arg \min_{\mathbf{u}_c} \left\{ \|\mathbf{u}_c\|_M^2 + \frac{h\lambda^*}{\lambda^* - h} \times \|\mathbf{A} \mathbf{u}_c - \mathbf{b}\|^2 + \lambda^* \phi^2(\mathbf{u}_c) \right\}. \quad (31)$$

Next, the outer minimization problem (31) is solved. To reduce the computation burden, the minimization problem, which is a vector optimization problem on  $\mathbf{u}_c$ , is converted to a one-dimensional search problem. For this purpose, the following function with two independent variables  $\mathbf{u}_c$  and  $\lambda$  is introduced

$$R(\mathbf{u}_c, \lambda) = \frac{h\lambda}{\lambda - h} \|\mathbf{A} \mathbf{u}_c - \mathbf{b}\|^2 + \lambda \phi^2(\mathbf{u}_c), \quad (32)$$

where  $\lambda$  belongs to the interval  $(h, +\infty)$ . Then, the cost of the inner maximization in (27) can be equal to the constrained minimization problem over the scalar  $\lambda$  [29],

$$L(\mathbf{u}_c) = \arg \min_{\lambda > h} R(\mathbf{u}_c, \lambda). \quad (33)$$

As a result, the original problem turns out to be equivalent to

$$\mathbf{u}_c = \arg \min_{\lambda > h} \min_{\mathbf{u}_c} J(\mathbf{u}_c, \lambda) \quad (34)$$

where  $J(\mathbf{u}_c, \lambda) = \|\mathbf{u}_c\|_M^2 + R(\mathbf{u}_c, \lambda)$ .

Taking derivative of  $J(\mathbf{u}_c, \lambda)$  with respect to  $\mathbf{u}_c$ , it yields

$$\left[ \mathbf{G}(\lambda) + \lambda \rho_A \left( \rho_A + \frac{\rho_b}{\|\mathbf{u}_c(\lambda)\|} \right) \mathbf{I}_n \right] \mathbf{u}_c(\lambda) = \mathbf{N}(\lambda) \quad (35)$$

where  $\mathbf{G}(\lambda) = \mathbf{M} + W(\lambda) \mathbf{A}^T \mathbf{A}$ ,  $\mathbf{N}(\lambda) = W(\lambda) \mathbf{A}^T \mathbf{b}$ , and  $W(\lambda) = \frac{h\lambda}{\lambda - h}$ . Then, for any nonzero  $\mathbf{u}_c$  in (35), we get

$$\mathbf{u}_c(\lambda) = \left[ \mathbf{G}(\lambda) + \lambda \rho_A \left( \rho_A + \frac{\rho_b}{\|\mathbf{u}_c(\lambda)\|} \right) \mathbf{I}_n \right]^{-1} \mathbf{N}(\lambda) \quad (36)$$

Define a scalar  $\xi = \|\mathbf{u}_c(\lambda)\|$ . Then, the equation (36) becomes

$$\xi^2 - \mathbf{N}^T(\lambda) \left[ \mathbf{G}(\lambda) + \lambda \rho_A \left( \rho_A + \frac{\rho_b}{\xi} \right) \mathbf{I}_n \right]^{-2} \mathbf{N}(\lambda) = 0. \quad (37)$$

It can be shown that a unique solution  $\xi^* > 0$  exists for (37) if  $\lambda \rho_A \rho_b < \|\mathbf{N}(\lambda)\|$ , and otherwise,  $\xi^* = 0$ , which means that  $\mathbf{u}_c(\lambda) = 0$ <sup>1</sup>. As a result, it is obtained that

$$\mathbf{u}_c^*(\lambda) = \left[ \mathbf{G}(\lambda) + \lambda \rho_A \left( \rho_A + \frac{\rho_b}{\xi^*} \right) \mathbf{I}_n \right]^{-1} \mathbf{N}(\lambda) \quad (38)$$

when  $\lambda \rho_A \rho_b \leq \|\mathbf{N}(\lambda)\|$ , and otherwise,  $\mathbf{u}_c^*(\lambda) = 0$ . Now, let  $J(\lambda)$  denote the minimum value of  $J(\mathbf{u}_c, \lambda)$  over  $\mathbf{u}_c$  in (34), i.e.,

$$J(\lambda) = \min_{\mathbf{u}_c} J(\mathbf{u}_c, \lambda) = J(\mathbf{u}_c^*(\lambda), \lambda) \\ = \|\mathbf{u}_c^*(\lambda)\|_M^2 + W(\lambda) \|\mathbf{A} \mathbf{u}_c^*(\lambda) - \mathbf{b}\|^2 + \lambda \phi^2(\mathbf{u}_c^*(\lambda)).$$

Finally, the unsaturated RobCA problem can be solved by determining  $\lambda^*$  from the following scalar-valued optimization problem

$$\lambda^* = \arg \min_{\lambda > h} J(\lambda). \quad (39)$$

Because the function  $J(\lambda)$  is unimodal [29], the minimization problem (39) is always well-posed such that an unique minimum on its domain is attainable.

In sum, the unsaturated RobCA algorithm is implemented as follows:

#### Inputs:

- $\hat{E}$  and  $\hat{u}$  are from the FDD scheme, and the virtual actuator torque  $\tau$  is from high-level controller.
- Choose the weighting parameters  $M$  and  $h$ .

#### Steps:

- 1) Solve the equation (37) and obtain the unique positive solution  $\xi^*$  by using numerical methods.
- 2) Solve the innermost minimization problem in (34) with respect to  $\mathbf{u}_c$ . The solution  $\mathbf{u}_c^*(\lambda)$  is given by

$$\mathbf{u}_c^*(\lambda) = \begin{cases} \left[ \mathbf{G}(\lambda) + \lambda \rho_A \left( \rho_A + \frac{\rho_b}{\xi^*} \right) \mathbf{I}_n \right]^{-1} \mathbf{N}(\lambda), & \text{if } \lambda \rho_A \rho_b < \|\mathbf{N}(\lambda)\| \\ 0, & \text{if } \lambda \rho_A \rho_b \geq \|\mathbf{N}(\lambda)\|. \end{cases} \quad (40)$$

- 3) Compute  $\lambda^*$  by solving the scalar-valued minimization problem defined in (39).
- 4) Substitute  $\lambda^*$  into (40) to get the solution  $\mathbf{u}_c = \mathbf{u}_c^*(\lambda^*)$ .

<sup>1</sup>The derivation of the condition  $\lambda \rho_A \rho_b \leq \|\mathbf{N}(\lambda)\|$  can be found in Appendix B of [29].

### B. Saturated Case

When actuator amplitude and rate constraints are considered, the RobCA defined in (25) can be converted into a second-order cone programming (SOCP) problem formulation. For the inner maximization problem in (25), using triangle inequality, it is noted that

$$\begin{aligned} & \|(\mathbf{A} + \Delta\mathbf{A})\mathbf{u}_c - (\mathbf{b} + \Delta\mathbf{b})\| \\ & \leq \|\mathbf{A}\mathbf{u}_c - \mathbf{b}\| + \|\Delta\mathbf{A}\|\|\mathbf{u}_c\| + \|\Delta\mathbf{b}\| \\ & \leq \|\mathbf{A}\mathbf{u}_c - \mathbf{b}\| + \rho_A\|\mathbf{u}_c\| + \rho_b, \end{aligned} \quad (41)$$

which provides an upper bound for  $\|(\mathbf{A} + \Delta\mathbf{A})\mathbf{u}_c - (\mathbf{b} + \Delta\mathbf{b})\|$ . In fact, this upper bound is achievable if  $\Delta\mathbf{A}$  and  $\Delta\mathbf{b}$  have forms of

$$\Delta\mathbf{A} = \frac{\mathbf{A}\mathbf{u}_c - \mathbf{b}}{\|\mathbf{A}\mathbf{u}_c - \mathbf{b}\|} \frac{\mathbf{u}_c^T}{\|\mathbf{u}_c\|} \rho_A, \quad \Delta\mathbf{b} = -\frac{\mathbf{A}\mathbf{u}_c - \mathbf{b}}{\|\mathbf{A}\mathbf{u}_c - \mathbf{b}\|} \rho_b. \quad (42)$$

Then, it follows that

$$\|(\mathbf{A} + \Delta\mathbf{A})\mathbf{u}_c - (\mathbf{b} + \Delta\mathbf{b})\| = \|\mathbf{A}\mathbf{u}_c - \mathbf{b}\| + \rho_A\|\mathbf{u}_c\| + \rho_b$$

which is the desired upper bound from the triangle inequality. Therefore, we may conclude that the maximum cost of the inner maximization problem can be given by

$$L(\mathbf{u}_c) = h(\|\mathbf{A}\mathbf{u}_c - \mathbf{b}\| + \rho_A\|\mathbf{u}_c\| + \rho_b)^2. \quad (43)$$

As a result, the RobCA problem reduces to

$$\begin{aligned} \mathbf{u}_c = \arg \min_{\underline{\mathbf{u}}_c \leq \mathbf{u}_c \leq \bar{\mathbf{u}}_c} & \left\{ \|\mathbf{u}_c\|_M^2 \right. \\ & \left. + h(\|\mathbf{A}\mathbf{u}_c - \mathbf{b}\| + \rho_A\|\mathbf{u}_c\| + \rho_b)^2 \right\}. \end{aligned} \quad (44)$$

The solution of problem (44) can be obtained by solving the following SOCP problem

$$\begin{aligned} & \min_{\mathbf{u}_c, t_i} t_1 \\ \text{subject to} & \begin{cases} \|col(t_2, t_3)\| \leq t_1 \\ \|\mathbf{M}^{1/2}\mathbf{u}_c\| \leq t_2 \\ \|\mathbf{A}\mathbf{u}_c - \mathbf{b}\| \leq \frac{t_3}{\sqrt{h}} - \rho_b - t_4 \\ \|\mathbf{u}_c\| \leq \frac{t_4}{\rho_A} \\ \underline{\mathbf{u}}_c \leq \mathbf{u}_c \leq \bar{\mathbf{u}}_c, \end{cases} \end{aligned} \quad (45)$$

where the variables  $t_i \in \mathbb{R}^+$  with  $i \in \{1, 2, \dots, 4\}$ , and  $col(t_2, t_3) \in \mathbb{R}^2$  is a column vector composed of the variables  $t_2$  and  $t_3$ . The above SOCP problem can be solved by using nonlinear optimization softwares, such as YALMIP, CVX, etc.

## V. SIMULATIONS

To study the effectiveness and performance of the proposed MRA high-level control scheme and the RobCA strategy, numerical simulations have been carried out for the rigid spacecraft attitude tracking system under actuator faults. The spacecraft is assumed to have the inertia matrix of  $\mathbf{J} = [20 \ 0 \ 0.9; 0 \ 17 \ 0; 0.9 \ 0 \ 15]$ . The external disturbances are assumed to be

$$\mathbf{d}(t) = \begin{bmatrix} 0.01 + 0.01 \cos(0.05t) \\ 0.01 \sin(0.08t) + 0.01 \cos(0.06t) \\ 0.01 + 0.015 \sin(0.06t) \end{bmatrix} \text{ N} \cdot \text{m}.$$

The initial attitude is  $\mathbf{Q}(0) = [0.2 \ -0.15 \ -0.25 \ 0.9354]^T$  with a zero initial angular velocity. The desired reference angular velocity is given as

$$\boldsymbol{\omega}_d(t) = 0.573 \times \left[ \cos\left(\frac{t}{40}\right) \sin\left(\frac{t}{30}\right) - \cos\left(\frac{t}{50}\right) \right]^T \text{ deg/s}.$$

For the consideration of practical application, the angular velocity is measured from a rate-integrating gyro [30] which is model as  $\tilde{\boldsymbol{\omega}}(t) = \boldsymbol{\omega}(t) + \boldsymbol{\beta}(t) + \boldsymbol{\eta}_v(t)$  and  $\dot{\boldsymbol{\beta}}(t) = \boldsymbol{\eta}_u(t)$ , where  $\tilde{\boldsymbol{\omega}}(t)$  is the gyro output, the vector  $\boldsymbol{\beta}(t)$  is gyro bias, and the vectors  $\boldsymbol{\eta}_v(t)$  and  $\boldsymbol{\eta}_u(t)$  are independent mean zero Gaussian white-noise process with spectral densities given by  $\sigma_v^2 \mathbf{I}_3$  and  $\sigma_u^2 \mathbf{I}_3$ , respectively. The covariance of  $\boldsymbol{\eta}_v(t)$  and  $\boldsymbol{\eta}_u(t)$  is given by  $E\{\boldsymbol{\eta}_v(t)\boldsymbol{\eta}_v^T(\tau)\} = \mathbf{I}_3\sigma_v^2\delta(t-\tau)$  and  $E\{\boldsymbol{\eta}_u(t)\boldsymbol{\eta}_u^T(\tau)\} = \mathbf{I}_3\sigma_u^2\delta(t-\tau)$ , where  $\delta(t-\tau)$  is the Dirac delta function [30]. Since discrete-time gyro measurements are employed in practice, based on the result from [31], the above continuous-time model is further equivalently convert to a discrete-time model in the simulation. The measurement bias of angular velocity sensor is 1 deg/h on each axis. Moreover, due to the limited manufacturing tolerances, the mounting misalignments of attitude sensor and angular velocity sensor in the simulation are assumed to be 0.005 deg and 0.1 deg, respectively.

In order to achieve three-axis control of a spacecraft, four reaction wheels in a pyramid configuration are considered as actuators, and both loss of effectiveness faults and additive faults are considered in actuators. The scenarios of time-varying actuator faults are described as follows.

- 1) The first reaction wheel experiences partial loss of control effectiveness with a time-varying effectiveness gain  $e_1 = 0.5 + 0.5e^{-t}$ .
- 2) The second reaction wheel undergoes an additive fault with  $\bar{u}_2 = -0.03 + 0.03e^{-0.5t} + 0.001\text{rand}(\cdot)$  N·m.
- 3) The third reaction wheel experiences loss of effectiveness and additive fault simultaneously with  $e_3 = 0.6 + 0.4e^{-0.5t}$  and  $\bar{u}_3 = -0.02 + 0.02e^{-t} + 0.002\text{rand}(\cdot)$  N·m, respectively.
- 4) The fourth reaction wheel undergoes a complete failure.

Here, the function  $\text{rand}(\cdot)$  generates a random value from the normal distribution with mean 0 and standard deviation 1.

The estimate of actuator fault information can be provided by an FDD scheme as developed in [32], where local observers are used to estimate fault-related parameters online for each of the actuators. The maximum imprecision in fault estimation is assumed to be 20%. The high-level controller parameters are chosen with  $\beta = 0.42$ ,  $k_1 = 7.5$ ,  $k_2 = 50$ ,  $k_3 = 0.5$ , and  $\Lambda_i = 0.8\mathbf{I}_2$ ,  $i \in \{1, 2, 3\}$ . For RobCA, the weighting matrix  $\mathbf{M}$  and weighting scalar  $h$  in (26) are  $\mathbf{M} = \mathbf{I}_4$  and  $h = 1 \times 10^4$ , respectively. To have an easy interpretation, attitude tracking errors are re-expressed in Euler angles. For the purpose of comparison, PD controller [26] with pseudoinverse based control allocation is also carried out.

Figs. 2 and 3 show the closed-loop system performance under MRA controller with unsaturated RobCA and PD controller with pseudoinverse control allocation, respectively. It is observed from Fig. 2 that the desired states can still be tracked

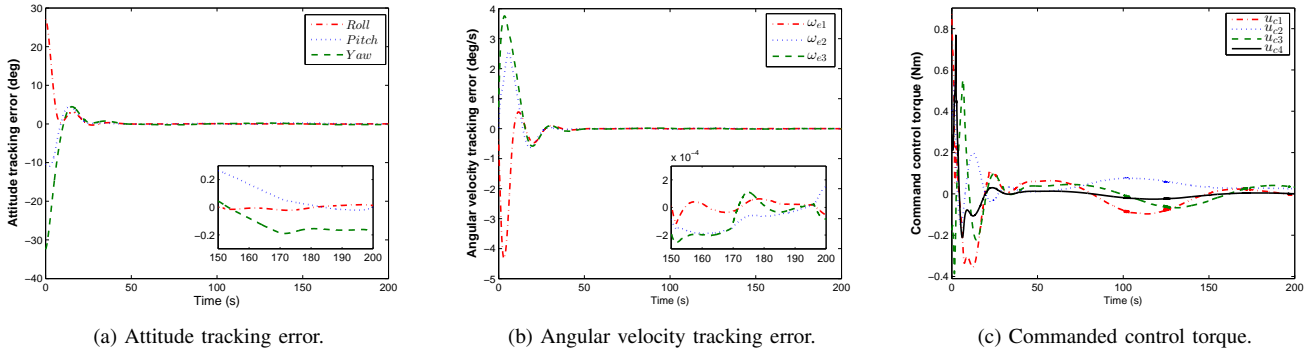


Fig. 2. System performance under MRA controller with unsaturated RobCA.

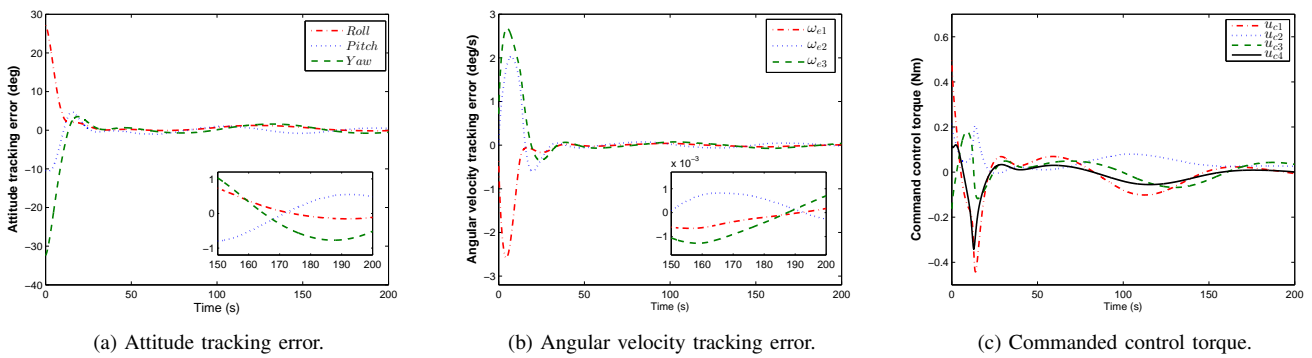


Fig. 3. System performance under PD controller with unsaturated pseudoinverse based control allocation.

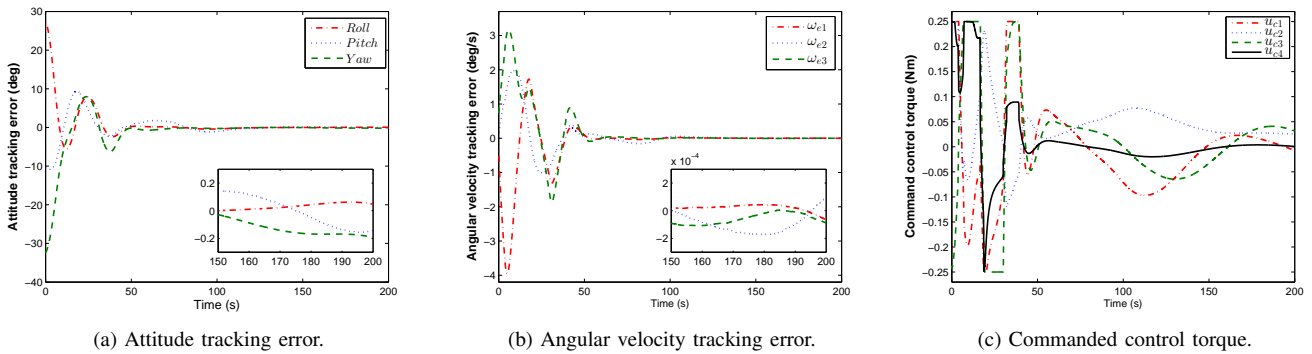


Fig. 4. System performance under MRA controller with saturated RobCA.

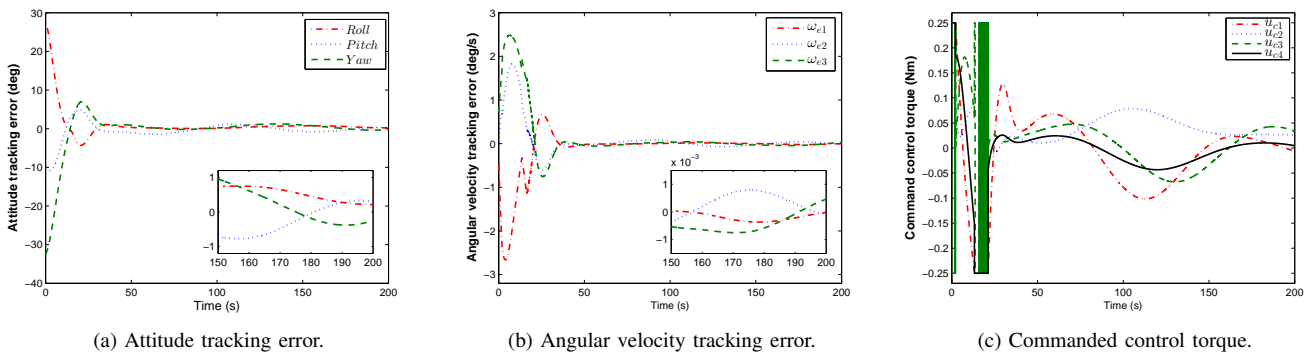


Fig. 5. System performance under PD controller with saturated pseudoinverse based control allocation.

with small tracking errors and a rapid convergence rate when the proposed scheme is used. Whereas for performance of the PD controller with pseudoinverse control allocation method in Fig. 3, due to the FDD imprecisions and external disturbances, the steady-state of attitude tracking error is about 1 deg and angular velocity tracking error is about  $1.5 \times 10^{-3}$  deg/s, which are much larger than that under the proposed scheme. This is due to the fact that the proposed scheme possesses some robustness with respect to the considered form of external disturbances in (2) and imprecise FDD estimation. However, it should be noted that degraded control performance may be observed if the actual disturbance frequencies in (2) cannot be estimated or measured accurately.

Next, the actuator saturation is taken into account in simulation. In this case, the limitations on the reaction wheel control torque are assumed to be  $\underline{u}_{ci} = -0.25$  N·m and  $\bar{u}_{ci} = 0.25$  N·m,  $i \in \{1, 2, 3, 4\}$ . Referring to Figs. 4 and 5, it is observed that steady-state tracking errors under the proposed scheme are still superior to that under the PD controller with pseudoinverse based control allocation method even in the presence of actuator saturation.

## VI. CONCLUSIONS

In this paper, the MRA high-level controller incorporating RobCA strategy has been proposed for spacecraft attitude tracking system in the presence of external disturbances, FDD imprecisions, and actuator saturation. First, an MRA controller is designed as the high-level controller to specify total control efforts such that the desired attitude trajectories can be followed asymptotically. Then, a RobCA scheme is further developed to distribute the total control command determined by the high-level controller to individual actuators. The RobCA problem is formulated as a min-max optimization problem and further converted to a scalar-valued optimization problem to reduce computation burden. The effectiveness of the proposed strategy are illustrated in simulation.

## REFERENCES

- [1] Godard, "Fault tolerant control of spacecraft," Ph.D. dissertation, Ryerson University, Toronto, Ontario, Canada, 2010.
- [2] Y. M. Zhang and J. Jiang, "Bibliographical review on reconfigurable fault-tolerant control systems," *Annual Reviews in Control*, vol. 32, no. 2, pp. 229–252, Dec. 2008.
- [3] W. C. Cai, X. H. Liao, and Y. D. Song, "Indirect robust adaptive fault-tolerant control for attitude tracking of spacecraft," *Journal of Guidance, Control, and Dynamics*, vol. 31, no. 5, pp. 1456–1463, Sep.–Oct. 2008.
- [4] J. Jin, S. Ko, and C. K. Ryoo, "Fault tolerant control for satellites with four reaction wheels," *Control Engineering Practice*, vol. 16, no. 10, pp. 1250–1258, Oct. 2008.
- [5] B. Xiao, Q. Hu, D. Wang, and E. K. Poh, "Attitude tracking control of rigid spacecraft with actuator misalignment and fault," *IEEE Transactions on Control Systems Technology*, vol. 21, no. 6, pp. 2360–2366, Nov. 2013.
- [6] D. Bustan, S. K. H. Sani, and N. Pariz, "Adaptive fault-tolerant spacecraft attitude control design with transient response control," *IEEE/ASME Transactions on Mechatronics*, vol. 19, no. 4, pp. 1404–1411, Aug. 2014.
- [7] J. D. Boskovic, S.-M. Li, and R. K. Mehra, "Intelligent control of spacecraft in the presence of actuator failures," in *Proc. 38th IEEE Conf. Decision Control*, vol. 5, Phoenix, AZ, 1999, pp. 4472–4477.
- [8] W. Chen and M. Saif, "Observer-based fault diagnosis of satellite systems subject to time-varying thruster faults," *Journal of Dynamic Systems, Measurement, and Control*, vol. 129, no. 3, pp. 352–356, May 2007.
- [9] B. Xiao, Q. Hu, and M. I. Friswell, "Active fault-tolerant attitude control for flexible spacecraft with loss of actuator effectiveness," *International Journal of Adaptive Control and Signal Processing*, vol. 27, no. 11, pp. 925–943, Nov. 2013.
- [10] T. Jiang, K. Khorasani, and S. Tafazoli, "Parameter estimation-based fault detection, isolation and recovery for nonlinear satellite models," *IEEE Transactions on Control Systems Technology*, vol. 16, no. 4, pp. 799–808, Jul. 2008.
- [11] B. Xiao, Q. Hu, W. Singhose, and X. Huo, "Reaction wheel fault compensation and disturbance rejection for spacecraft attitude tracking," *Journal of Guidance, Control, and Dynamics*, vol. 36, no. 6, pp. 1565–1575, Nov.–Dec. 2013.
- [12] T. A. Johansen and T. I. Fossen, "Control allocation—a survey," *Automatica*, vol. 49, no. 5, pp. 1087–1103, May 2013.
- [13] J. J. Burken, P. Lu, Z. Wu, and C. Bahm, "Two reconfigurable flight-control design methods: Robust servomechanism and control allocation," *Journal of Guidance, Control, and Dynamics*, vol. 24, no. 3, pp. 482–493, May–Jun. 2001.
- [14] A. Casavola and E. Garone, "Fault-tolerant adaptive control allocation schemes for overactuated systems," *International Journal of Robust and Nonlinear Control*, vol. 20, no. 17, pp. 1958–1980, Nov. 2010.
- [15] H. Alwi and C. Edwards, "Fault tolerant control using sliding modes with on-line control allocation," *Automatica*, vol. 44, no. 7, pp. 1859–1866, Jul. 2008.
- [16] M. T. Hamayun, C. Edwards, and H. Alwi, "Design and analysis of an integral sliding mode fault-tolerant control scheme," *IEEE Transactions on Automatic Control*, vol. 57, no. 7, pp. 1783–1789, Jul. 2012.
- [17] Q. Shen, D. Wang, S. Zhu, and E. K. Poh, "Inertia-free fault-tolerant spacecraft attitude tracking using control allocation," *Automatica*, vol. 62, pp. 114–121, Dec. 2015.
- [18] L. Cui and Y. Yang, "Disturbance rejection and robust least-squares control allocation in flight control system," *Journal of Guidance, Control, and Dynamics*, vol. 34, no. 6, pp. 1632–1643, Nov.–Dec. 2011.
- [19] Q. Hu, B. Li, D. Wang, and E. K. Poh, "Velocity-free fault-tolerant control allocation for flexible spacecraft with redundant thrusters," *International Journal of Systems Science*, vol. 46, no. 6, pp. 976–992, 2015.
- [20] M. J. Sidi, *Spacecraft Dynamics and Control*. Cambridge, U.K.: Cambridge, NY: Cambridge University Press, 1997.
- [21] Z. Chen and J. Huang, "Attitude tracking and disturbance rejection of rigid spacecraft by adaptive control," *IEEE Transactions on Automatic Control*, vol. 54, no. 3, pp. 600–605, Mar. 2009.
- [22] A. Sanyal, A. Fosbury, N. Chaturvedi, and D. Bernstein, "Inertia-free spacecraft attitude tracking with disturbance rejection and almost global stabilization," *Journal of Guidance, Control, and Dynamics*, vol. 32, no. 4, pp. 1167–1178, Jul.–Aug. 2009.
- [23] O. Härkegard and S. T. Glad, "Resolving actuator redundancy-optimal control vs. control allocation," *Automatica*, vol. 41, no. 1, pp. 137–144, 2005.
- [24] W. Luo, Y.-C. Chu, and K.-V. Ling, "Inverse optimal adaptive control for attitude tracking of spacecraft," *IEEE Transactions on Automatic Control*, vol. 50, no. 11, pp. 1639–1654, Nov. 2005.
- [25] M. Krstic, I. Kanellakopoulos, and P. Kokotovic, *Nonlinear and adaptive control design*. New York: Wiley, 1995.
- [26] J. T. Y. Wen and K. Kreutz-Delgado, "The attitude control problem," *IEEE Transactions on Automatic Control*, vol. 36, no. 10, pp. 1148–1162, Oct. 1991.
- [27] M. Benosman and K. Y. Lum, "Online references reshaping and control reallocation for nonlinear fault tolerant control," *IEEE Transactions on Control Systems Technology*, vol. 17, no. 2, pp. 366–379, Mar. 2009.
- [28] V. H. Nascimento and A. H. Sayed, "Optimal state regulation for uncertain state-space models," in *Proc. Amer. Control Conf.*, 1999, pp. 419–424.
- [29] A. Sayed, V. Nascimento, and F. Cipparrone, "A regularized robust design criterion for uncertain data," *SIAM Journal on Matrix Analysis and Applications*, vol. 23, no. 4, pp. 1120–1142, 2002.
- [30] R. L. Farrenkopf, "Analytic steady-state accuracy solutions for two common spacecraft attitude estimators," *Journal of Guidance, Control, and Dynamics*, vol. 1, no. 4, pp. 282–284, 1978.
- [31] F. Markley and J. Crassidis, *Fundamentals of Spacecraft Attitude Determination and Control*. New York, NY: Springer, pp. 147, 2014.
- [32] D. Wang, E. K. Poh, S. Zhu, Q. Shen, and B. Wu, "Active fault tolerant control for satellite attitude maneuver," Nanyang Technological University, Tech. Rep., Apr. 2014.